Journal of Information Systems Engineering and Management
2025, 10(4)
e-ISSN: 2468-4376
https://www.jisem-journal.com/

Research Article

Thiourea-Assisted Deposition of Cadmium Sulfide Thin Films: Structural and Optical Analysis

Zoubir Becer[1], Dahmane Djendaoui[2], Abdellatif Laib[1] Azzeddine Beggas[1]
[1]*Laboratoire d'intelligence artificielle et de ses applications (LIAP), University of El-Oued, Address: B.P. 789 39000 El-Oued 39000, Algeria*
[2]*Laboratory Applied Automation and Industrial Diagnostics (LAADI), University of Djelfa: Djelfa 17000, Algeria*

ARTICLE INFO

Received: 21 Feb 2025
Revised: 27 Feb 2025
Accepted: 29 Mar 2025
Published: 23 May 2025

ABSTRACT

In this study, cadmium sulfide (CdS) thin films were grown on glass substrates via chemical bath deposition, with a focus on how varying thiourea doses influence film formation. Structural analysis revealed that all samples crystallized in a cubic zinc blende phase; however, increasing thiourea content led to marked reductions in grain size (55.67 nm to 11.34 nm) and overall crystallinity. Concurrently, microstrain and dislocation density exhibited notable increases (from 0.62×10^(-3) to 3.0×10^(-3) and from 0.32×10^(-3) lines/nm² to 7.7×10^(-3) lines/nm² respectivaly) , indicating degradation in crystalline quality and the emergence of lattice imperfections. Morphological assessment revealed reduced grain connectivity and enhanced surface disorder at higher thiourea levels. Optical characterization showed a progressive blue shift in the transmission spectra, increased transmittance, and a widening of the optical band gap from 1.80 eV to 1.96 eV. The Urbach energy rose from 0.2 eV to 0.5 eV, while the refractive index decreased with increasing precursor dose. These findings demonstrate that thiourea serves as a critical parameter for modulating both structural integrity and optoelectronic performance in CdS thin films, supporting their tunability for advanced photonic and photovoltaic applications.

Keywords: Cadmium Sulfide (CdS) Thin Films, Chemical Bath Deposition (CBD), Thiourea Dose, Crystallinity, Optical Band Gap, Microstrain, Dislocation Density, Urbach Energy, Refractive Index, Optoelectronic Materials

1. INTRODUCTION

Among semiconductor thin film materials, cadmium sulfide (CdS) stands out as a particularly promising n-type window layer for photovoltaic technologies, especially in thin-film solar cell architectures like p-CdTe and chalcopyrite-based systems including p-$CuInSe_2$ and p-$Cu(In,Ga)Se_2$ (CIGS) (Contreras. et al, 2002; Sui. et al, 2021). Its exceptional utility stems from remarkable optoelectronic characteristics, including exceptional optical transparency and low electrical resistance (Chopra. et al, 1979; Sulka. et al, 2023).

Characterized by a wide and direct bandgap transition of 2.42 eV, CdS demonstrates high electron affinity and intrinsic n-type conductivity (Battisha. et al, 2002), rendering it versatile for numerous electronic and optoelectronic device applications (Ilieva. et al, 1999). Researchers have developed multiple synthesis techniques for CdS thin films, encompassing approaches like spray pyrolysis (Aschour, 2003; Falcony. et al, 2018), sputtering (Islam. et al, 2013), electrodeposition (Raffaelle. et al, 1999), vacuum evaporation (Senthil. et al, 2001), and chemical bath deposition (CBD) (Oliva. et al, 2001; Beggas. et al, 2019).

Among these fabrication methodologies, chemical bath deposition emerges as a particularly attractive technique. This method offers significant advantages, including simplified processing, cost-effectiveness, lower temperature requirements compared to vacuum-based approaches, and the capacity to produce high-quality films under optimized growth conditions. Historically, CBD has been instrumental in CdS thin film deposition since the early 1960s (Kitaev. et al, 1965).

The primary objective of this research is to comprehensively examine how thiourea dose influences the structural and optical characteristics of CdS thin films synthesized via chemical bath deposition, utilizing $CdSO_4$ as the

Journal of Information Systems Engineering and Management
2025, 10(4)
e-ISSN: 2468-4376
https://www.jisem-journal.com/

Research Article

cadmium ion precursor. Section II details the experimental procedure and deposition methodology. Section III presents comprehensive results and discussion, examining: (A) Structural Properties through X-ray diffraction, (B) Optical Properties via UV-Vis spectroscopy, and (C) Chemical composition using FTIR spectroscopy. The concluding section synthesizes key findings and discusses their implications for optoelectronic applications.

2. EXPERIMENTAL PROCEDURE

Cadmium sulfide (CdS) thin films were synthesized through the chemical bath deposition (CBD) method, employing four distinct doses of thiourea as the sulfur source. Standard microscope glass slides (dimensions: 75 mm × 25 mm × 1.1 mm) served as deposition substrates. Prior to film growth, the substrates underwent a sequential cleaning process involving acetone immersion, rinsing with deionized water, and ambient air drying. The deposition bath was formulated using cadmium sulfate as the cadmium ion source and thiourea for sulfur, with ammonia functioning as a complexing agent to stabilize metal ions in solution. Specific chemical bath compositions corresponding to the four sample sets are detailed in Table 1. The precursor solution was magnetically stirred for 45 minutes to ensure homogeneity before the substrates were vertically immersed. The bath temperature was maintained at 55 °C, and the films were allowed to grow undisturbed for 60 minutes without stirring. Post-deposition, the substrates were withdrawn, thoroughly rinsed with deionized water, and air-dried. The resulting CdS films exhibited a uniform yellow appearance and adhered well to the glass surfaces. Adherence was qualitatively assessed by gentle scratching using fingernails and a fine-edged tool, which confirmed good mechanical bonding of the films to the substrates.

The crystallographic structure of the synthesized CdS films was analyzed using an XPERT-PRO X-ray diffractometer equipped with CuKα radiation (λ = 1.54060 Å), operated at an accelerating voltage of 40 kV and a current of 40 mA. Diffraction patterns were recorded over a 2θ range spanning from 20° to 70° to identify the predominant crystal phases. To investigate the optical band gap, UV–visible spectroscopy was employed across the spectral range of 300 to 900 nm using a Shimadzu UV-1800 spectrophotometer. Additionally, Fourier transform infrared (FT-IR) spectroscopy was conducted with a Shimadzu IR Affinity-1 instrument, covering a wavenumber interval of 400–4000 cm^{-1} to examine the vibrational modes and chemical bonding characteristics of the deposited films.

Table (1): The dose of the chemicals used in the bath for the preparation of the CdS samples.

Samples	Compositions			
	$CdSO_4$ (g)	$CS(NH_2)_2$ (g)	NH_3 (ml)	Thiourea Dose (mmol/l)
CdS1	0.275	0.095	2	0.025
CdS2	0.275	0.190	2	0.050
CdS3	0.275	0.285	2	0.075
CdS4	0.275	0.380	2	0.100

3. RESULTS AND DISCUSSION

3.1. Structural Properties

3.1.1. Crystallinity and Grain Size

Figure 1 presents the X-ray diffraction (XRD) profiles of CdS thin films synthesized at a controlled bath temperature of 55 °C with a fixed deposition duration of 60 minutes. A distinct diffraction peak centered around 2θ ≈ 26.7° is evident, corresponding to the (111) lattice plane of the zinc blende (cubic) phase, indicating a preferential growth orientation. This structural assignment aligns with prior findings reported by Zhai et al. (2005), Oladeji et al. (2002), and Ichimura et al. (1999), who similarly identified cubic CdS structures across various deposition approaches. Although cadmium sulfide can adopt both hexagonal (wurtzite) and cubic (sphalerite) phases depending on the synthesis route, the hexagonal configuration is generally thermodynamically favored, as noted by Pradhan et al. (2007). Importantly, the wurtzite phase is often preferred in photovoltaic applications due to a closer lattice match

Journal of Information Systems Engineering and Management
2025, 10(4)
e-ISSN: 2468-4376
https://www.jisem-journal.com/

Research Article

with CuInSe2 (1.2%) compared to the mismatch presented by the cubic variant (0.7%). The intensity of the (111) peak was observed to increase with lower thiourea doses, suggesting improved crystallinity, likely due to enhanced film thickness. Conversely, at elevated thiourea levels, the absence of discernible diffraction peaks implies either poor crystalline development or insufficient film thickness for detection by XRD.

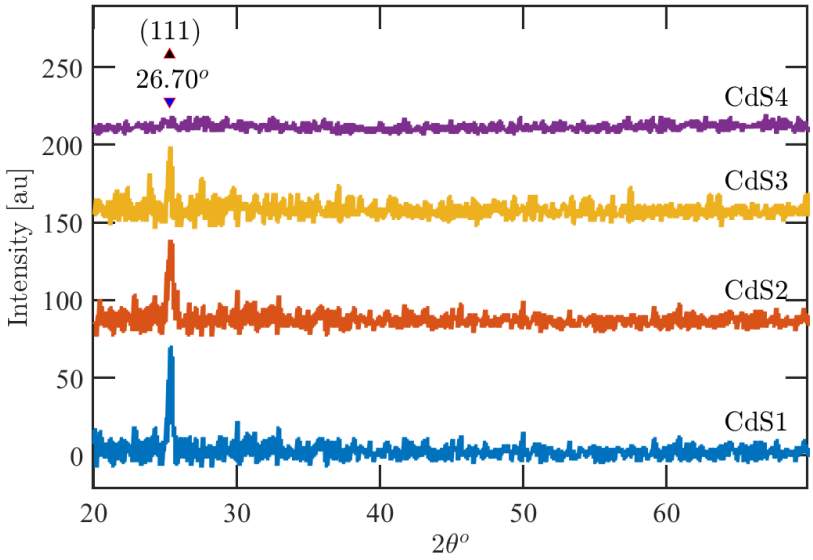

Figure 1. X-ray diffraction patterns of CdS thin films

Crystallite size was inferred from the broadening characteristics of the X-ray diffraction peaks, based on the principle that broader peaks correspond to smaller crystallite dimensions, as originally described by Cullity et al. (1956). The interplanar spacing (d_{hkl}) was computed using Bragg's Law:

$$n\lambda = 2d_{hkl}\ sin\ sin\ \theta \quad (1)$$

In this equation, n denotes the diffraction order (typically 1), λ represents the X-ray wavelength and θ is the Bragg diffraction angle. The calculated d −spacings, corresponding to 2θ Bragg's angles of prominent values of the major diffraction peaks, and additional structural parameters are summarized in Table 2. To determine the lattice constant (a) for the cubic phase of CdS, the standard relationship for cubic symmetry was applied:

$$\frac{1}{d^2} = \frac{h^2 + k^2 + l^2}{a^2} \quad (2)$$

where (h, k, l) are the Miller indices of the reflecting planes. This equation enables the extraction of precise unit cell dimensions from XRD data for materials exhibiting cubic crystal systems.

Table (2): Structure parameters extracted from XRD patterns analysis.

Sample	2θ (°)	hkl	d_{hkl} (Å)	FWHM(°)	a (Å)
CdS1	26.7	(111)	3.34	0.151	5.76
CdS2	26.7	(111)	3.34	0.258	5.76
CdS3	26.7	(111)	3.34	0.719	5.76
CdS4	--	--	--	--	--

3.1.2. Strain and Dislocation

The crystallite size (D) of CdS nanoparticles was determined from the X-ray diffraction data using the Debye-Scherrer equation:

Journal of Information Systems Engineering and Management
2025, 10(4)
e-ISSN: 2468-4376
https://www.jisem-journal.com/

Research Article

$$D = \frac{K\,\lambda}{\beta\ cos\ cos\ (\theta)} \quad (3)$$

Here, $\lambda = 0.15418\,nm$ denotes the wavelength of CuKα radiation, K is a shape-dependent constant typically taken as 0.94, θ is the Bragg diffraction angle, and β refers to the full width at half maximum (FWHM) of the dominant peak, expressed in radians.

As presented in Table 3 and illustrated in Figure 2, increasing the thiourea dose led to a marked reduction in grain size—from 55.67 nm to 11.34 nm—indicating enhanced nucleation and finer nanocrystal formation under sulfur-rich conditions. These particles also exhibited a more uniform size distribution and improved colloidal stability.

While an ideal crystal structure is a theoretical construct rarely realized in practice, many engineering materials approximate crystalline order well enough to support reliable property prediction. Real-world crystals inherently possess structural defects such as microstrain and dislocations, which can be quantified from XRD patterns. These parameters are critical for assessing mechanical integrity and electronic behavior in device applications. The internal microstrain (δ) and dislocation density (δ) were calculated using the following relationships:

$$\varepsilon = \frac{\beta\ cos\ cos\ \theta}{4} \quad (4)$$

$$\delta = \frac{1}{D^2} \quad (5)$$

Both microstrain and dislocation density were found to increase with higher thiourea doses, likely as a consequence of decreased crystallite size and thinner film deposition. As depicted in Figure 2, this inverse relationship between crystallite size and strain further supports the notion that lattice imperfections become more pronounced in finer nanostructured films.

Table (3): Various structural parameters calculated for CdS thin films for different thiourea doses.

Sample	Crystallite size D (Å)	Lattice strain, ε ($\times 10^{-3}$)	Dislocation density, δ ($\times 10^{-3}$ lines nm^{-2})
CdS1	55.670	0.62	0.32
CdS2	27.726	1.25	1.30
CdS3	11.346	3.00	7.77
CdS4	--	--	--

Journal of Information Systems Engineering and Management
2025, 10(4)
e-ISSN: 2468-4376
https://www.jisem-journal.com/

Research Article

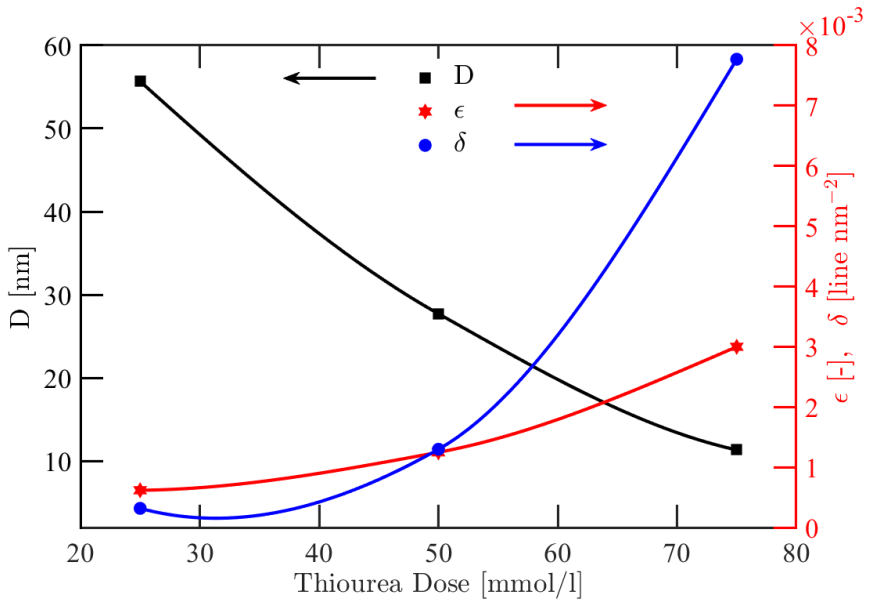

Figure 2. Variation of crystallite size and micro strain as a function of thiourea dose.

3.2. Optical properties of the CdS thin films

3.2.1. Transmittance and Band Gap Energy

Figure 3 illustrates the spectral transmittance behavior of CdS thin films prepared with varying thiourea doses, recorded across the ultraviolet-visible range. A high level of transmittance is observed beyond 500 nm for all films, indicating significant transparency in the visible spectrum. However, as the thiourea dose increases, a decline in transmittance is apparent in the longer wavelength region. This attenuation can be attributed to enhanced film thickness and surface irregularities, both of which contribute to increased photon scattering and absorption.

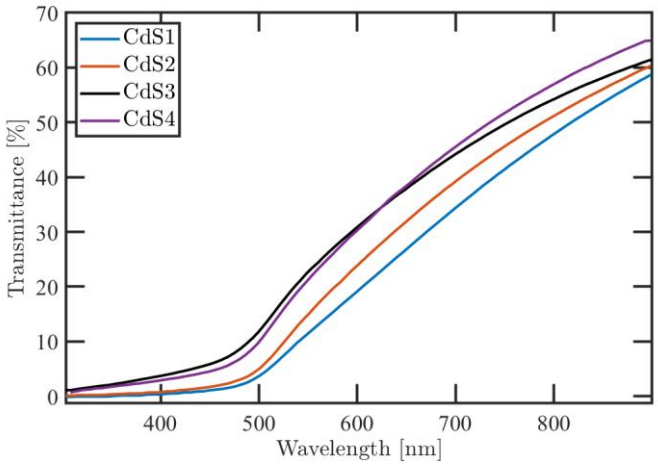

Figure 3. Optical transmission spectra of CdS thin films deposited with different thiourea dose.

Determining the optical band gap—a key parameter for semiconductors employed in optoelectronic applications—was achieved by analyzing the absorption spectra through Tauc plots. For direct band gap materials such as CdS, the band gap energy (E_g) was extracted by plotting $(\alpha h\vartheta)^2$against the photon energy ($h\vartheta$),

$$\alpha h\vartheta = A\left(h\vartheta - E_g\right)^{1/2} \quad (6)$$

where (α) represents the absorption coefficient. The intercept of the extrapolated linear region with the energy axis $h\vartheta$ yields the band gap value. The extracted band gap energies for different thiourea doses are compiled in Table 4.

Journal of Information Systems Engineering and Management
2025, 10(4)
e-ISSN: 2468-4376
https://www.jisem-journal.com/

Research Article

The observed trend reveals a narrowing of the optical band gap as the thiourea content increases, consistent with reported values in the literature. This reduction is likely related to changes in film morphology and crystallinity, which influence the electronic structure of the material.

3.2.2. Urbach Energy and Disorder

The emergence of an absorption tail near the band edge in the optical spectra of the CdS thin films suggests the presence of structural irregularities and localized disorder within the material. This phenomenon can be quantitatively characterized by the Urbach energy (E_u), which serves as a measure of the degree of disorder in the electronic structure of the films. E_u is determined from the exponential region of the absorption coefficient curve using the relation:

$$\alpha = \alpha_0 \, exp\left(\frac{h\vartheta}{E_u}\right) \tag{7}$$

where again, α is the absorption coefficient, and α_0 is a material-specific constant. The value of Urbach energy is extracted from the inverse slope of the linear portion of the $log\ (\alpha)$ versus photon energy plot.

The calculated band gap energies for CdS films grown with varying thiourea levels are presented in Table 4, while Figure 4 illustrates how both the band gap and Urbach energy change in response to thiourea dose. An increase in E_u with higher precursor doses indicates elevated structural disorder, which may arise from enhanced defect density or non-uniform grain growth during film formation.

Table (4): The estimated band gap and Urbach energy values for different thiourea dose

Sample	Eg (eV)	Eu (ev)
CdS1	1.96	0.2
CdS2	1.90	0.35
CdS3	1.85	0.42
CdS4	1.80	0.5

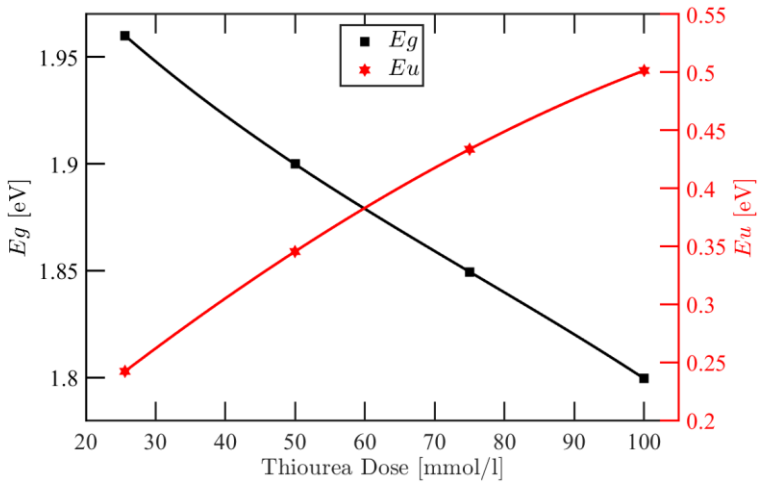

Figure 4. Evolution of the Urbach and the band gap energies as function of the thiourea dose dose

From Figure.4 it's clear that the optical gap in the obtained films is governed by the disorder.

3.2.3. Refractive Index and Extinction Coefficient

The optical constants of the CdS thin films; namely, the refractive index (n) and the extinction coefficient (k), as well as the film thickness (d), were determined through a rigorous spectral optimization method applied to transmission spectra. The methodology employed a least-squares minimization approach, expressed by the error function

Journal of Information Systems Engineering and Management
2025, 10(4)
e-ISSN: 2468-4376
https://www.jisem-journal.com/

Research Article

$$(\Delta T)^2 = \left|T_{Theory}(d,n,k,\lambda) - T_{Exp}\right|^2,$$

where T_{Exp} represents the experimentally measured transmission values as a function of wavelength (λ), and T_{Theory} denotes the transmission calculated using the Transfer-matrix method (Katsidis; Siapkas, 2002). The optimization algorithm systematically varied the optical parameters to minimize the spectral deviation between theoretical and experimental transmission data.

The retrieved film thicknesses for the four samples varied systematically, ranging from 221.55 nm in Sample 1 to 247.84 nm in Sample 4, with intermediate values of 238.39 nm and 241.85 nm for Samples 2 and 3, respectively. This progressive increase in film thickness correlates with the variations in thiourea dose during the chemical bath deposition process.

Figure 5 demonstrates the exceptional concordance between experimental transmission measurements and theoretically estimated values following the optimization process. The wavelength-dependent variations of the refractive index (n) and extinction coefficient (k), illustrated in Figure 6, validate the effectiveness of the employed characterization technique in elucidating the intrinsic optical properties of the CdS thin films.

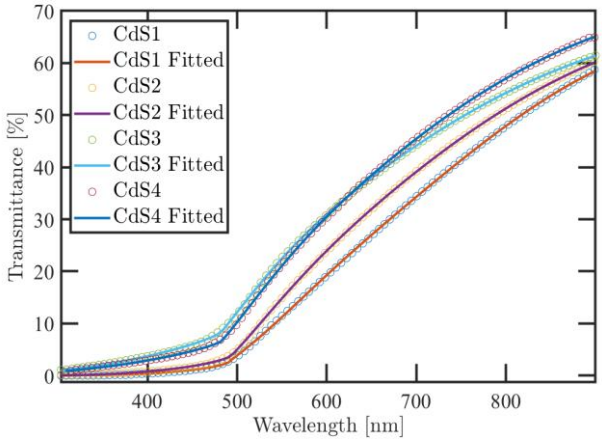

Figure 5. Concordance between experimental transmission measurements and theoretically estimated values.

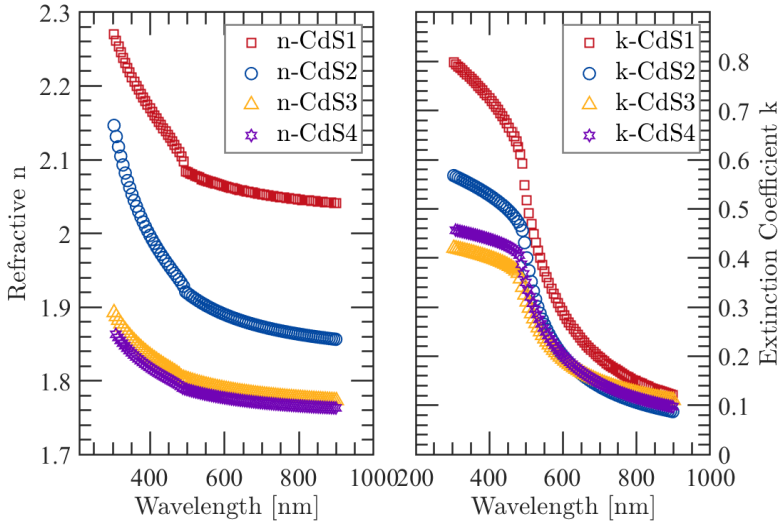

Figure 6. Estimated optical constants for CdS thin films: the refractive index (n) and the extinction coefficient (k) as a function of wavelength.

Journal of Information Systems Engineering and Management
2025, 10(4)
e-ISSN: 2468-4376
https://www.jisem-journal.com/

Research Article

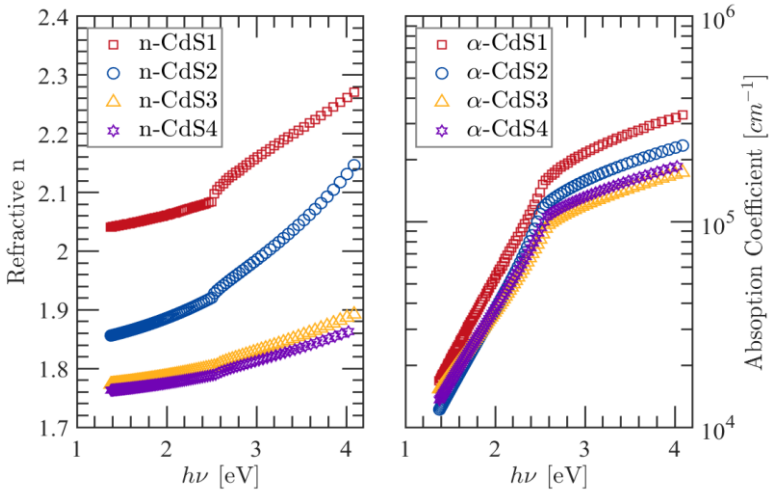

Figure 7. Estimated absorption coefficients along with refractive index as a function of photon energy.

3.3. Chemical composition using FTIR spectroscopy measurements

Figure 8 illustrates the FTIR spectra recorded at room temperature for the synthesized CdS thin films. A noticeable and broad absorption feature around 3443 cm^{-1} is observed, which corresponds to the O–H stretching vibrations. This spectral feature is typically associated with water molecules adsorbed onto the film surface. Its presence indicates that the samples may have absorbed moisture from the surrounding environment, likely due to their exposure to air following deposition.

In addition, the FTIR spectrum shows prominent peaks in the low wavenumber region, specifically around 391 cm^{-1}, 410 cm^{-1}, and 465 cm^{-1}, which are characteristic of the Cd-S stretching vibration in CdS (cadmium sulfide). These peaks confirm that CdS is the dominant phase in the thin film, as expected from the chemical bath deposition process. The presence of CdS is further supported by the lack of significant peaks in the mid and high wavenumber regions that would suggest a large amount of contamination.

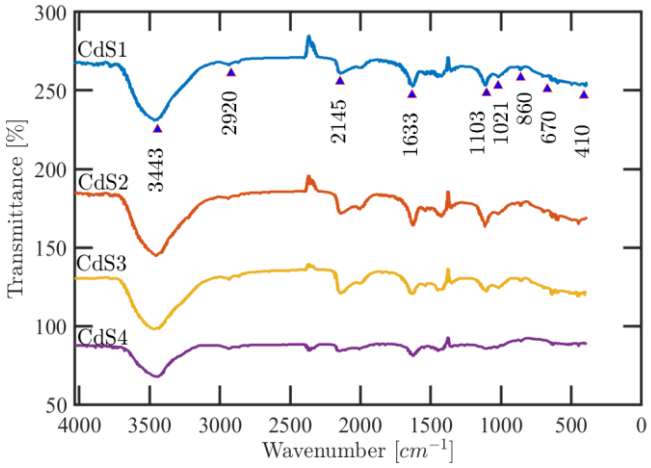

Figure 8. FTIR spectra of all CdS thin films obtained of different thiourea doses.

4. CONCLUSION

This study investigated the effect of thiourea dose on the structural and optical properties of CdS thin films prepared via chemical bath deposition (CBD). X-ray diffraction (XRD) revealed that lower thiourea doses produced films with better crystallinity and larger grain sizes (up to 55.67 nm), while higher doses resulted in smaller grains (down to 11.34 nm), increased micro strain, and higher dislocation density, indicating reduced structural quality. Optical

analysis showed a blue shift in transmission spectra and higher transmittance with increasing thiourea doses. The optical band gap widened from 1.80 eV to 1.96 eV, while the Urbach energy increased from 0.2 eV to 0.5 eV, reflecting deterioration of films quality.

The CdS thin films show a systematic thickness increase from 221.55 nm in Sample 1 to 247.84 nm in Sample 4, with intermediate values of 238.39 nm and 241.85 nm for Samples 2 and 3. This trend correlates with variations in thiourea dose during deposition. Additionally, the refractive index decreases with higher thiourea content.

These findings demonstrate that adjusting thiourea dose can effectively tune the structural and optical properties of CdS thin films, making them suitable for various optoelectronic applications. Lower thiourea doses are ideal for better crystalline quality, whereas higher doses may be advantageous for applications requiring larger band gaps or specific optical characteristics. Future research could focus on optimizing additional deposition parameters and integrating these films into device architectures.

REFERENCES

[1] Contreras, M., Romero, M., To, B., Hasoon, F., Noufi, R., Ward, S., & Ramanathan, K. (2002). Optimization of CBD CdS process in high-efficiency Cu(In,Ga)Se2-based solar cells. *Thin Solid Films, 403–404*, 204–211. https://doi.org/10.1016/S0040-6090(01)01538-3

[2] Sui, M., Chu, Y., & Zhang, R. (2021). A review of technologies for high efficiency silicon solar cells. *Journal of Physics: Conference Series, 1907*, 012026. https://doi.org/10.1088/1742-6596/1907/1/012026

[3] Chopra, K. L., & Das, S. R. (1979). *Thin film solar cells*. Plenum Press.

[4] Sulka, G. D. (2023). Electrochemistry of thin films and nanostructured materials. *Molecules, 28*(10), 4040. https://doi.org/10.3390/molecules28104040

[5] Battisha, I. K., Afify, H. H., Abd El-Fattah, G., & Badr, Y. (2002). *Phizika A, 11*, 31.

[6] Ilieva, M., Dimova-Malinovska, D., Ranguelov, B., & Markov, I. (1999). High temperature electrodeposition of CdS thin films on conductive glass substrates. *Journal of Physics: Condensed Matter, 11*(49), 10025–10031. https://doi.org/10.1088/0953-8984/11/49/320

[7] Aschour, A. (2003). Physical properties of spray pyrolysed CdS thin films. *Turkish Journal of Physics, 17*(8), 551–558.

[8] Falcony, C., Aguilar-Frutis, M. A., & García-Hipólito, M. (2018). Spray pyrolysis technique; high-K dielectric films and luminescent materials: A review. *Micromachines, 9*(8), Article 414. https://doi.org/10.3390/mi9080414

[9] Islam, M. A., Hossein, M. S., Aliyu, M. M., Chelvanathan, P., Huda, Q., Karim, M. R., Sopian, K., & Amin, N. (2013). Fabrication of CdS thin film using chemical bath deposition method. *Energy Procedia, 33*, 203–213. https://doi.org/10.1016/j.egypro.2013.05.059

[10] Raffaelle, R. P., Forsell, H., Potdevin, T., Fridefeld, R., Mantovani, J. G., Bailey, S. G., Hubbard, S. M., Gordon, E. M., & Hepp, A. F. (1999). CuInSe2 solar cells efficiency optimization. *Solar Energy Materials and Solar Cells, 57*, 167–178. https://doi.org/10.1016/S0927-0248(98)00172-X

[11] Senthil, K., Mangalaraj, D., & Narayandass, S. K. (2001). Structural and optical properties of CdS thin films. *Applied Surface Science, 169–170*, 476–479. https://doi.org/10.1016/S0169-4332(00)00732-7

[12] Oliva, A. I., Solis-Canto, O., Castro-Rodriguez, R., & Quintana, P. (2001). Formation of the band gap energy on CdS thin films growth by two different techniques. *Thin Solid Films, 391*, 28–35. https://doi.org/10.1016/S0040-6090(01)00830-6

[13] Beggas, A., Becer, Z., Ahmim, R., & Msaida, M. S. (2019). Structural and optical properties of PbS thin films deposited by chemical bath. *Defect and Diffusion Forum, 397*, 125–140. https://doi.org/10.4028/www.scientific.net/DDF.397.125

[14] Kitaev, G., Uritskaya, A., & Mokrushin, S. (1965). *Russian Journal of Physical Chemistry, 39*, 1101.

[15] Zhai, R., Wang, S., Xu, H., Wang, H., & Yan, H. (2005). Rapid formation of CdS, ZnS thin films by microwave-assisted chemical bath deposition. *Materials Letters, 59*(12), 1497–1501. https://doi.org/10.1016/j.matlet.2005.01.008

Research Article

[16] Oladeji, O., Chow, L., Liu, J. R., Chu, W. K., Bustamante, A. N. P., Fredricksen, C., & Schulte, A. F. (2000). Comparative study of CdS thin films deposited by single, continuous, and multiple dip chemical processes. *Thin Solid Films, 359*(2), 154–159. https://doi.org/10.1016/S0040-6090(99)00747-6

[17] Ichimura, M., Goto, F., & Arai, E. (1999). Structural and optical characterization of CdS films grown by photochemical deposition. *Journal of Applied Physics, 85*(10), 7411–7417. https://doi.org/10.1063/1.369371

[18] Pradhan, B., Sharma, A. K., & Ray, A. K. (2007). Conduction studies on chemical bath deposition nanocrystalline CdS thin films. *Journal of Crystal Growth, 304*(2), 388–392. https://doi.org/10.1016/j.jcrysgro.2007.03.041

[19] Cullity, B. D. (1956). *Elements of X-ray diffraction*. Addison-Wesley Publishing Company.

[20] Katsidis, C. C., & Siapkas, D. I. (2002). General transfer-matrix method for optical multilayer systems with coherent, partially coherent, and incoherent interference. *Applied Optics, 41*(19), 3978–3987. https://doi.org/10.1364/AO.41.003978